European Review for Medical and Pharmacological Sciences 2023; 27: 5973-5984

Value of pelvic ultrasound combined with pituitary MRI in diagnosis of central precocious puberty in girls

Y.-E. CHEN[1], X.-L. GU[2], L.-L. SHEN[1], M. XU[1]

[1]Department Ultrasonography, Nantong First People's Hospital, Jiangsu, China
[2]Department Radiology, Nantong First People's Hospital, Jiangsu, China

Abstract. – OBJECTIVE: This study aimed to investigate the value of pelvic ultrasound combined with pituitary magnetic resonance imaging (MRI) based on an artificial intelligence algorithm in the diagnosis of girls with central precocious puberty (CPP), providing reference for the prevention and control of CPP in girls.

PATIENTS AND METHODS: 75 girls with CPP and 75 normal girls in Nantong First People's Hospital were studied. Pelvic ultrasound parameters were compared between the two groups based on an artificial intelligence algorithm. Pituitary MRI parameters were analyzed, and pituitary function parameters were explored.

RESULTS: The results showed that the diagnostic sensitivity, specificity, and accuracy of the convolutional neural network (CNN) algorithm were 72.3%, 74.6%, and 78.3%, respectively. The sensitivity, specificity, and accuracy of CNN algorithm were significantly higher ($p<0.05$). The long diameter, anteroposterior diameter, and transverse diameter of the uterus in the precocious puberty (PP) group were significantly larger than those in the normal group (NG). The ovarian long diameter, ovarian anteroposterior diameter, and ovarian transverse diameter in PP group were significantly larger than those in NG. Uterine volume and ovarian volume in PP group were clearly higher than those in NG. The largest follicle diameter was clearly larger in PP patients than in NG patients. The coronal height, coronal width, sagittal height, and sagittal anteroposterior diameter of PP group were clearly higher than those of NG ($p<0.05$). The sagittal cross-sectional area of pituitary MRI morphology in PP group was significantly greater than that in NG. The pituitary MRI morphology pituitary volume was 272.68 mm in PP group and 191.37 mm in NG, and the pituitary volume was clearly larger in PP group than in NG. The pituitary function parameters estradiol (E_2), luteinizing hormone (LH) peak, follicle-stimulating hormone (FSH) peak, and LH peak/FSH peak were greater in PP group than in NG.

CONCLUSIONS: In summary, the uterine size and ovarian size of girls and the pituitary function index in PP group were larger. Pelvic ultrasound and pituitary MRI indexes can better diagnose CPP and can be widely used in clinical practice with positive diagnostic value.

Key Words:
Artificial intelligence algorithm, Safety medical imaging, Pelvic ultrasound, Pituitary MRI, Diagnostic value.

Introduction

With the change of people's diet and living habits, many children have poor eating habits and less exercise time, resulting in an increasing number of children with precocious puberty (PP). In recent years, the age range of onset of PP has also been expanding, and many young children have also developed PP, seriously affecting normal life[1]. PP can affect children's normal life and change their living habits[2]. PP is influenced by age, sex, race, lifestyle, living environment, etc. The common clinical manifestations of PP patients are early puberty and early secondary sexual characteristics; PP causes early cessation of the development of the relevant tissues and organs of children, which will significantly affect the growth and development of children, thus affecting the physical health of children[3-5]. As a special group, children with PP have abnormal physical development, great impact on psychological status, and have greater psychological pressure and anxiety, which is not conducive to the stability of physical status and the smooth progress of treatment[6,7]. Children with PP are vulnerable to rejection by other children of the same age, affecting normal socialization and life, thereby increasing the degree of depression in children and being not conducive to the normal physical development of patients. Therefore, children with PP require early diagnosis, prompting patients to receive targeted treatment, controlling PP, and promoting the normal development of the body[8].

Corresponding Author: Xiaolin Gu, MD; e-mail: gxiaolin258@163.com

Abnormal sex hormone levels are the intrinsic cause of PP, and both peripheral and central factors can cause increased sex hormone levels, and early detection and treatment are of great significance for children with PP. Early intervention and treatment of the disease should be performed to prevent the severity of PP and cause negative effects on the physiological function of patients[9,10]. Hypothalamic-pituitary-gonadal axis dysfunction is the pathogenesis of central precocious puberty (CPP); therefore, the detection of pituitary function and structure is an important method for the diagnosis of PP[11]. The most common current examination methods include ultrasonography, magnetic resonance imaging (MRI), and pituitary function index examination[12]. Safe medical imaging is essential in children and can prevent instrumental examination from affecting children's growth and development[13]. Ultrasonography has the advantages of high safety, simplicity and convenience, high patient acceptance, non-invasive convenience, and clear results, and is widely used in clinical practice. Ultrasonography can rapidly and effectively diagnose the patient's uterine and ovarian conditions and has a positive guiding value[14,15]. Pituitary MRI is a common clinical examination method of pituitary gland structure and function, which can prevent the examination from causing radiation to children. It is a standard imaging technique for the diagnosis of PP. It can observe the pituitary gland structure and function in real time, which is easy to apply, non-invasive, and easy to repeat. It has become an important examination tool for early identification of PP in children and has positive value in the diagnosis and disease evaluation of PP[16,17]. In recent years, artificial intelligence has been widely used in clinical medicine, providing convenience for clinical diagnosis and treatment[18,19]. Deep learning algorithms have achieved great success in computer vision fields such as image classification and target detection[20]. Convolutional neural network (CNN) algorithm has unique advantages in image recognition, image transformation of ultrasound and MRI, can achieve the prediction of PP, and provide artificial intelligence support for PP diagnosis[21,22].

The value of pelvic ultrasound combined with pituitary MRI in the diagnosis of girls with CPP based on computational intelligence system and safe medical imaging was explored. The pelvic ultrasound parameters of girls with PP were compared with normal girls. The differences in pituitary MRI measurements between the two groups were analyzed. The pituitary function parameters of the two groups were compared, providing guidance and reference for the prevention and treatment of girls with PP.

Patients and Methods

Study Subjects

75 girls with CPP and 75 normal girls admitted to Nantong First People's Hospital from January 2020 to December 2020 were selected as the study subjects to analyze the value of pelvic ultrasound combined with pituitary MRI in the diagnosis of girls with CPP.

Method

According to the general data of the two groups, the mean age of girls in PP group was 7.45±2.28 years, the mean age of girls in normal group (NG) was 7.29±2.86 years; the BMI of girls in PP group was 17.47±2.16 kg/m^2, and that in NG group was 17.19±2.26 kg/m^2. There was no statistical difference in the mean age, BMI between girls in PP group and NG (p>0.05), with comparability. This study was approved by the Medical Ethics Committee of Nantong First People's Hospital.

Inclusion criteria: (1) complete medical records; (2) patients older than 5 years old; (3) patients with no contraindications to ultrasound and MRI examination; (4) patients with a high degree of cooperation; (5) patients and their families signed informed consent.

Exclusion criteria: (1) patients with other vital organ diseases; (2) patients with malignant tumors; (3) patients with genetic diseases; (4) patients with communication disorders; (5) patients with contraindications to ultrasound and MRI examination; (6) patients who are unwilling to participate in this trial.

Pelvic ultrasonography and pituitary MRI were performed in 150 girls. Color Doppler ultrasonography was used and a convex array probe and a linear array probe with frequencies of 2-7 MHz were configured. Girls were placed in the supine position with fully filled bladder, and their long diameter, anteroposterior diameter, and transverse diameter were measured in the sagittal and coronal sections of the ovaries and uterus; if multiple follicles were found, the diameter of the largest follicle among them was measured; based

on support vector machine (SVM) algorithm and CNN algorithm for ultrasonic image processing and analysis.

Pituitary MRI was performed on all girls using a superconducting magnetic resonance apparatus (SuperMark 1.5T, Shanghai Huantong Science and Education Equipment Co., Ltd., Shanghai, China) with an 8-channel phase-controlled cranial coil and a fast spin echo (FSE) sequence. Its parameters were set as follows: the repetition time was 2,400 ms, the matrix was 320 to 160, and the slice thickness was 3 mm. Coronal and sagittal T1-weighted (T1WI) images of the skull were measured.

The levels of estradiol (E_2), luteinizing hormone (LH), and follicle stimulating hormone (FSH) were measured by immunochemical chemiluminescence.

The method flow is shown in Figure 1.

Outcome Measures

(1) Statistical analysis of general information of PP group and NG, mainly including gender, mean age, and BMI, BMI calculation method is given in Equation (1).

$$BIM = \frac{Weight}{Height^2}$$

(2) The diagnostic effect of PP girls under different algorithms was compared, the main indicators are Accuracy, Precision, and Recall, and the calculation method is shown in Equations (2)-(4). TP represents the number of PP girls correctly predicted by the algorithm; TN indicates the number of non-PP girls correctly predicted by the algorithm; FP indicates the number of non-PP girls predicted as PP girls by the algorithm; FN represents the number of PP girls predicted as non-PP girls.

$$Accuracy = \frac{TP+TN}{TP+TN+FP+FN}$$

$$Precision = \frac{TP}{TP+FP}$$

$$Recall = \frac{TP}{TP+FN}$$

(3) Uterine and ovarian conditions of PP group and NG, mainly including the long diameter, anteroposterior diameter, and transverse diameter of uterus and ovary.

(4) The morphological parameters of pituitary MRI in two groups mainly including coronal height diameter, coronal width diameter, sagittal height diameter, sagittal anteroposterior diameter, sagittal cross-sectional area, and pituitary volume.

(5) Pituitary function indexes, mainly E_2, LH peak, FSH peak, and LH peak/FSH peak, were observed.

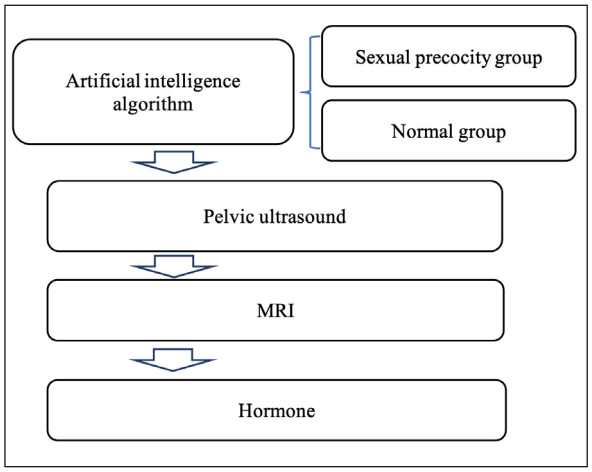

Figure 1. Flow diagram of method.

Statistical Analysis

SPSS 20.0 (IBM Corp., Armonk, NY, USA) was adopted for data statistics and analysis. Mean±standard deviations (±s) represented measurement data and *t*-test was adopted. Count data were presented as percentages (%), and χ^2 test was used. A p-value <0.05 was considered statistical significance.

Results

Processing Analysis of Pelvic Ultrasound Images and Pituitary MRI Images in Patients with CPP

Figure 2 shows the processing analysis of pelvic ultrasound images and pituitary MRI images of CPP patients, A and D are the original images, B and E are the images processed by the support vector machine (SVM) algorithm, and C and F are the images processed by the CNN algorithm. Both SVM and CNN algorithms can improve the definition of the image and make the structure clearer.

A Comparative Analysis of Diagnostic Effect of Two Artificial Intelligence Algorithms

Figure 3 shows the comparative analysis of the diagnostic sensitivity under the two algorithms. The diagnostic sensitivity under SVM

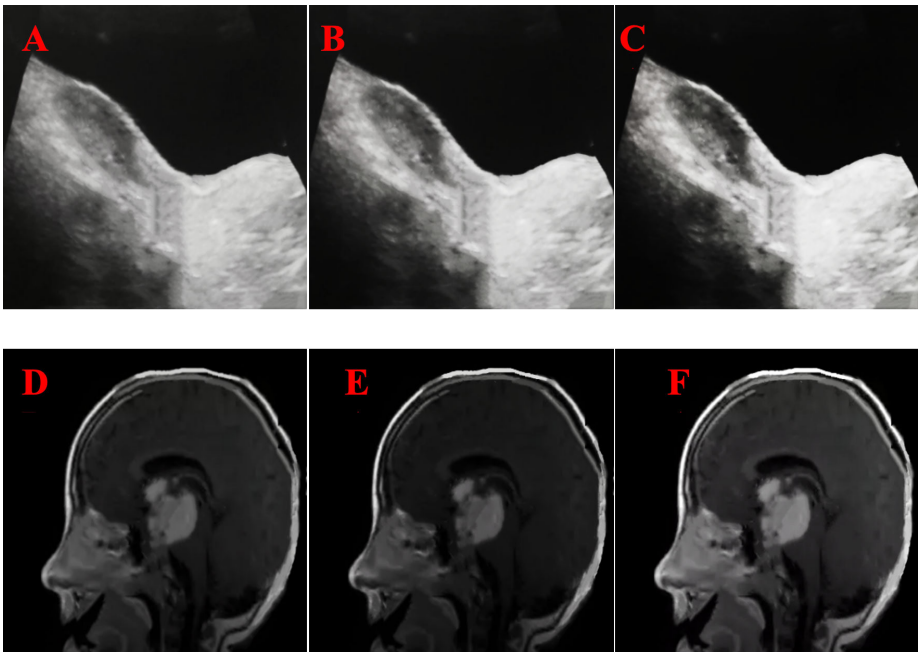

Figure 2. Processing analysis of pelvic ultrasound and pituitary MRI images. (**A**) and (**D**), are original images, (**B**) and (**E**) processed by SVM algorithm, and (**C**) and (**F**) processed by CNN algorithm). (Patient, Female, CPP).

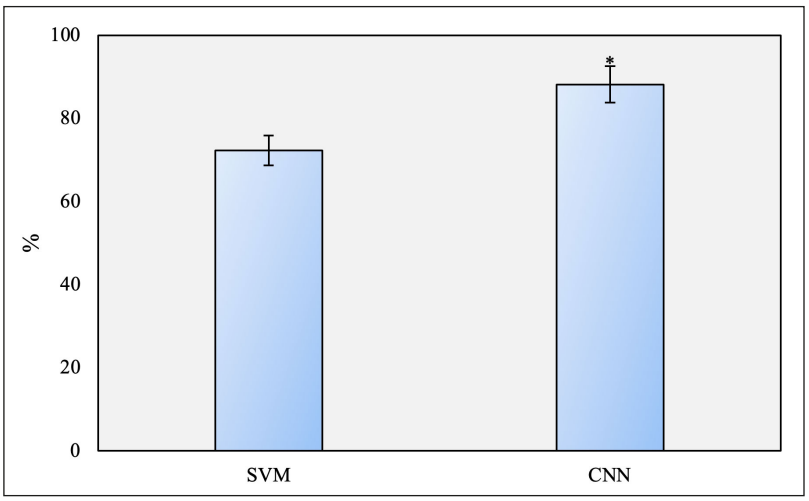

Figure 3. Comparative analysis of diagnostic sensitivity under two algorithms. (*p<0.05 compared with SVM algorithm).

algorithm was 72.3%, and the diagnostic sensitivity under CNN algorithm was 88.2%. The diagnostic sensitivity of CNN algorithm was higher (p<0.05).

Figure 4 shows the comparison of diagnostic specificity between the two algorithms. The diagnostic specificity was 74.6% under SVM algorithm and 86.7% under CNN algorithm. The diagnostic specificity of CNN algorithm was higher (* indicates p<0.05).

Figure 5 indicates the comparison of diagnostic accuracy under the two algorithms. The diagnostic accuracy was 78.3% under SVM algorithm and 89.7% under CNN algorithm. It can be found that the diagnostic accuracy of CNN algorithm was higher (* indicates p<0.05).

Uterine and Ovarian Status of Patients in Two Groups

Figure 6 indicates the size of the uterus of patients in PP group and NG. The long diameter of the uterus of patients was 2.38 cm, the anteroposterior diameter of the uterus was 0.87 cm, the transverse diameter of the uterus was 1.62 cm in PP group; and those in NG was 1.97 cm, 0.79 cm, and 1.28 cm. The long diameter of the uterus, the anteroposterior diameter of the uterus, and the transverse diameter of the uterus in PP group were clearly greater than those in NG (* indicates p<0.05).

Figure 7 suggests the ovarian size of patients in PP group and NG. The ovarian long diameter, anteroposterior diameter, and transverse diameter of PP group were 2.32 cm, 1.08 cm, and 1.15 cm, respectively;

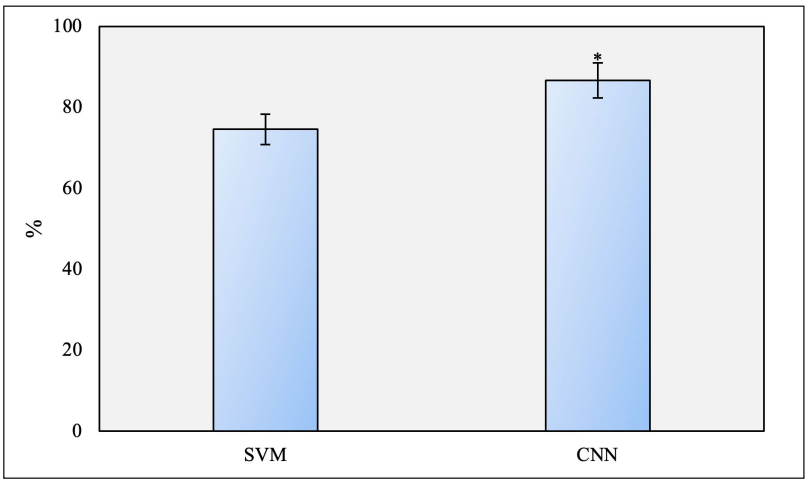

Figure 4. Comparison of diagnostic specificity under two algorithms. (*p<0.05).

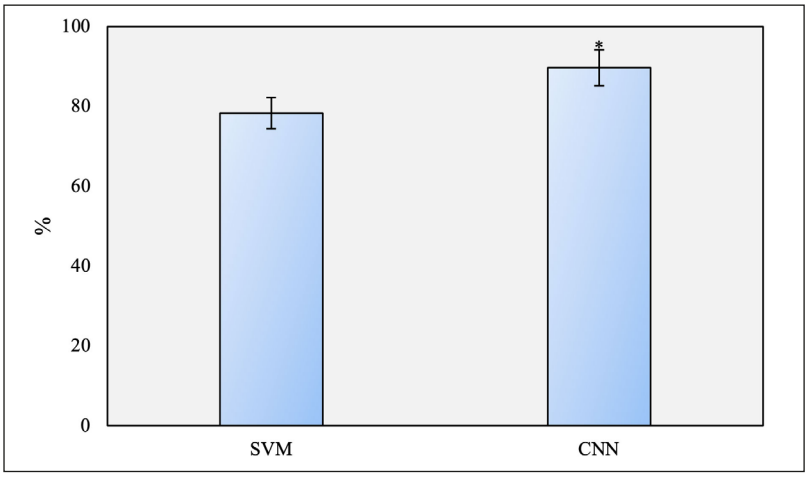

Figure 5. Comparison of diagnostic accuracy under two algorithms. (*p<0.05).

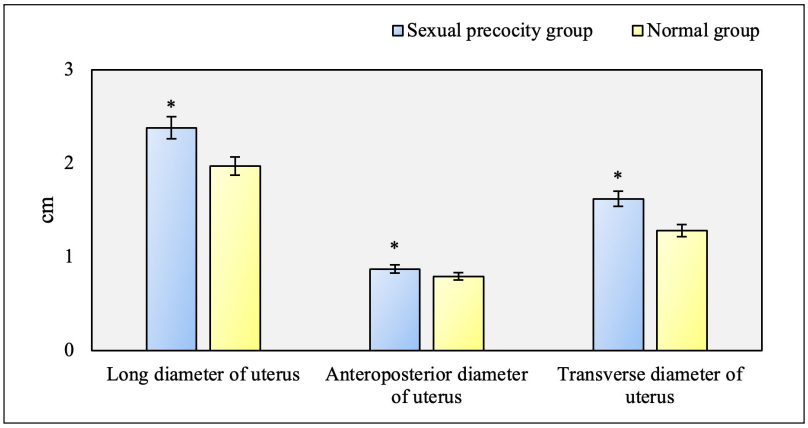

Figure 6. Analysis of uterine size in patients. (*p<0.05 compared with NG).

and those of NG patients were 1.93 cm, 1.02 cm, and 1.07 cm, respectively. The ovarian long diameter, anteroposterior diameter, and transverse diameter of PP group were greater (* indicates p<0.05).

Figure 8 illustrates the uterine and ovarian volumes of patients. The uterine volume was 1.92 cm^3, the ovarian volume was 1.71 cm^3 in PP group; and those in NG was 1.19 cm^3 and 1.08 cm^3. The uterine volume and ovarian volume of PP group were greater (* indicates p<0.05).

Figure 9 illustrates the analysis of the maximum follicle diameter of the patients. The maximum follicle diameter of the PP group was 0.73 cm. The maximum follicle diameter of the NG was 0.25 cm. The maximum follicle diameter of the PP group was larger (* indicates p<0.05).

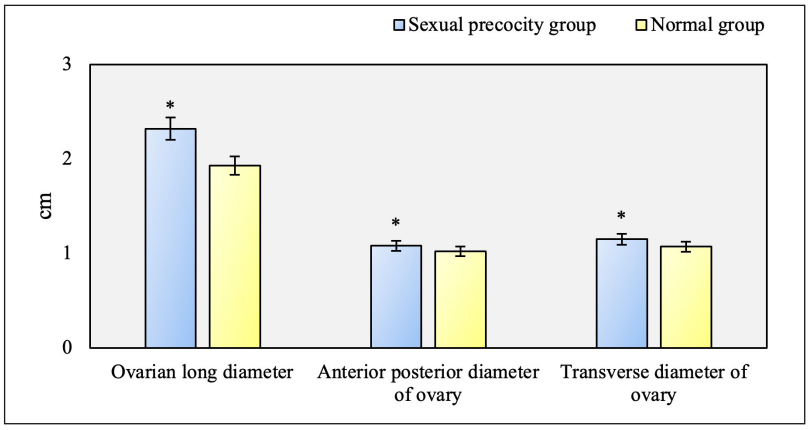

Figure 7. Ovarian size in patients. (*p<0.05).

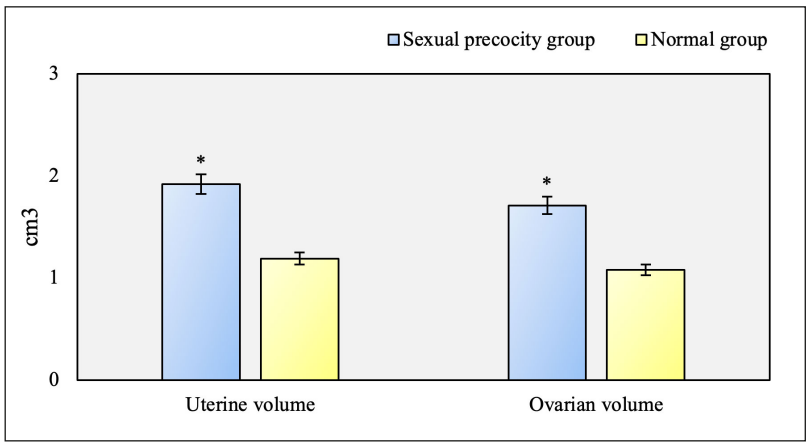

Figure 8. Uterine and ovarian volume analysis in patients. (*p<0.05).

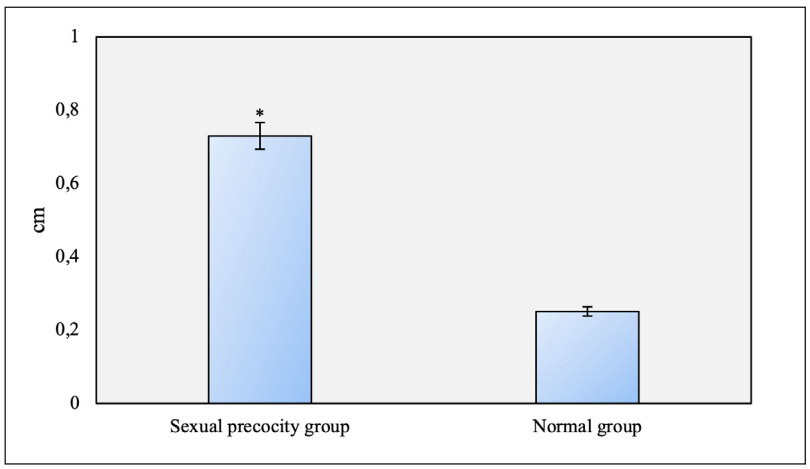

Figure 9. Maximum follicle diameter in patients. (*p<0.05).

Pituitary MRI Morphological Parameters

Figure 10 illustrates the morphological parameters of pituitary MRI in patients. In PP group, the coronal height diameter was 5.17 mm, the coronal width diameter was 12.78 mm, the sagittal height diameter was 5.19 mm, the sagittal anteroposterior diameter was 7.44 mm; and those in NG was 4.59 mm, 11.37 mm, 4.68 mm, and 6.87 mm. The coronal height diameter, coronal width diameter, sagittal height diameter, and sagittal anteroposterior diameter in PP group were greater (* indicates p<0.05).

Figure 11 illustrates the sagittal cross-sectional area of pituitary MRI morphology in patients. The sagittal cross-sectional area of pituitary MRI morphology was 36.72 mm in PP group and 33.45 mm in NG. Therefore, the sagittal cross-sectional area of pituitary MRI morphology in PP group was larger (* indicates p<0.05).

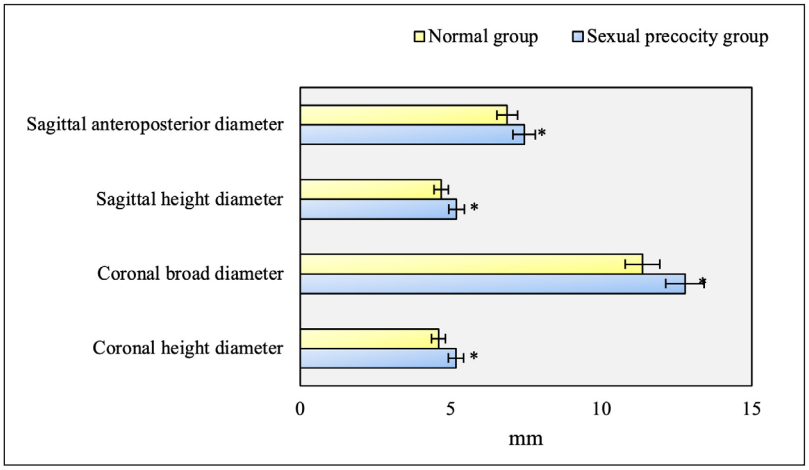

Figure 10. Pituitary MRI morphological parameters in patients. (*p<0.05).

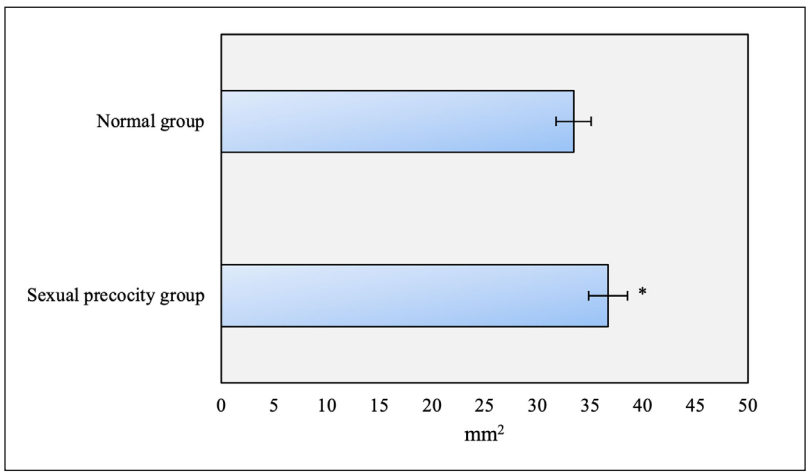

Figure 11. Morphological sagittal cross-sectional area of pituitary MRI in patients. (*p<0.05).

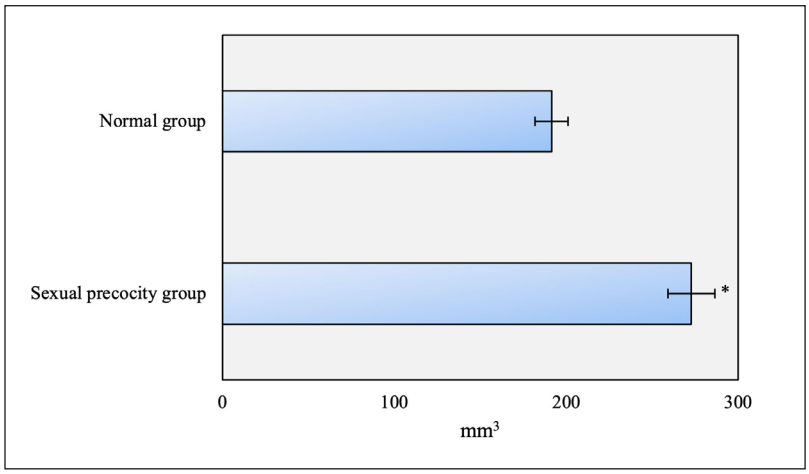

Figure 12. Pituitary MRI morphology pituitary volume in patients. (*p<0.05).

Figure 12 suggests the pituitary MRI morphology pituitary volume of the patients. The pituitary MRI morphology pituitary volume of the PP group was 272.68 mm, and that of the NG was 191.37 mm. Therefore, the pituitary volume of the PP group was larger (* indicates p<0.05).

Function index analysis of pituitary

Figure 13 illustrates the pituitary function index E_2 of the patients. The pituitary function index E_2 of the PP group was 8.12 mm; and that of the NG was 5.56 mm. The pituitary function index E_2 of the PP group was greater (* indicates p<0.05).

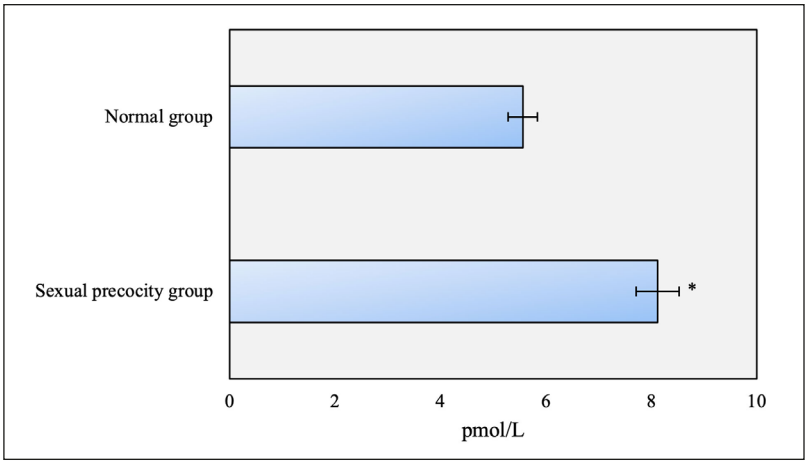

Figure 13. Analysis of pituitary function index E_2 in patients. (*p<0.05).

Figure 14 suggests the analysis of LH and FSH peaks in patients' pituitary function indexes. In PP group, LH peak was 12.78 mIU/L, FSH peak was 13.78 mIU/L; and that in NG was 4.27 mIU/L and 10.65 mIU/L. LH and FSH peaks in PP group were greater (* indicates p<0.05).

Figure 15 shows the analysis of the results of pituitary function index LH peak/FSH peak. It was found that the pituitary function index LH peak/FSH peak was 0.93 in PP group and 0.4 in NG. The pituitary function index LH peak/FSH peak was greater in PP group (* indicates p<0.05).

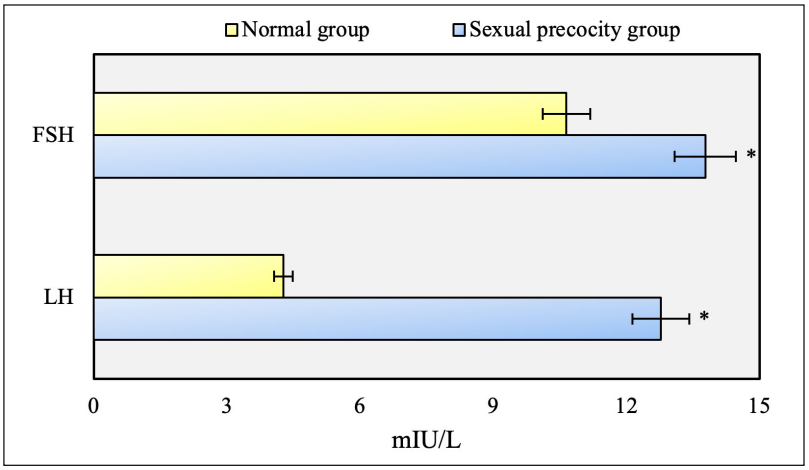

Figure 14. Analysis of pituitary function parameters LH and FSH peaks in patients. (*p<0.05).

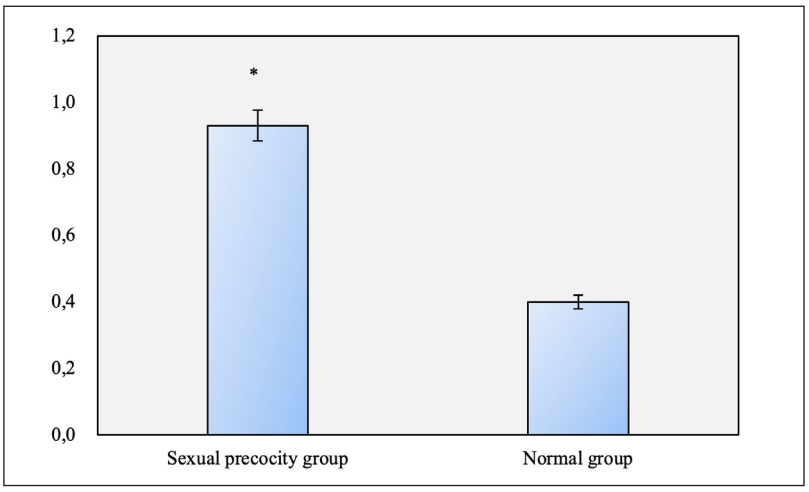

Figure 15. Analysis of pituitary function parameters LH peak/FSH peak in patients. (*p<0.05).

Discussion

PP is the phenomenon of early puberty due to abnormal sex hormone levels in children leading to abnormal growth and development of children. At present, the prevention and control of PP in children is a research hotspot in the field of medicine[23]. Children with PP will experience symptoms of rapid physical growth, early maturation of reproductive organs, and early onset of sexual characteristics. Adolescent characteristics can accompany children, affect the daily life of children, bring many inconveniences to children, affect the physical fitness of patients, and reduce the immunity of patients. Fail to timely and effectively control the disease easily causes adverse phenomena such as tissue and organ failure[24,25]. PP will not only affect the physical health of children, but also affect the psychological status and daily life of children, the PP characteristics of children will be rejected by peers, seriously affecting the normal life and social activities of children[26]. Drug therapy is the most important treatment for PP, different drugs control and alleviate the disease through different mechanisms of action, regulate hormone levels in children, and early diagnosis and treatment have positive clinical significance in preventing and blocking PP[27]. Pelvic ultrasound is of high value in the diagnosis and evaluation of PP in children, and changes in ultrasound parameters and indicators have guiding significance for the diagnosis of PP in children[28]. CPP has been affected by pituitary function, and the study of pituitary function structure is conducive to the prevention and diagnosis of PP. Pituitary MRI, as a diagnostic method for PP, has a good application value and can assess the pituitary status and function of children and provide a reference for the diagnosis of PP[29,30]. The treatment of pelvic ultrasound and pituitary MRI based on a deep learning model is beneficial to improve the diagnostic efficiency and accuracy and provide technical support for the prevention of diseases.

Pelvic ultrasound indicators, pituitary MRI indicators, and pituitary function indicators will have a certain impact on PP, which has guiding significance for the evaluation of PP in children and is widely used in clinical practice[31]. In the pituitary MRI images of girls with CPP, abnormal pituitary signal is also one of the common manifestations. Signal abnormalities may be related to pathological changes of pituitary cells, such as fatty degeneration and fibrosis. Different types of signal abnormalities may be associated with different etiologies and clinical features. Increased posterior pituitary thickness is one of the common MRI features of CPP[32]. This may be related to abnormal activation of the hypothalamic-pituitary-adrenal axis and increased secretion of vasopressin. Changes in the thickness of the posterior pituitary gland can be used as an auxiliary indicator of CPP, which is helpful for enhanced scanning and exclusion of pituitary tumors. For girls with CPP with abnormal pituitary gland shape, enhanced scan can be used to rule out pituitary tumors and other causes. Enhanced scans can provide more detailed information on blood supply and perfusion, helping to determine the abnormal nature of pituitary structures. Pituitary tumors are uncommon in CPP but still need to be ruled out to ensure proper diagnosis and treatment. Studies have shown that pituitary MRI can also be used to predict the effect and prognosis of CPP. Pituitary MRI indicators such as the thickness of the posterior pituitary gland and abnormal pituitary signal are related to treatment response and prognosis. These indicators can help doctors evaluate the patient's condition and the choice of treatment strategies, and guide subsequent follow-up and management[33]. The diagnosis of CPP requires a comprehensive consideration of clinical manifestations, growth and development, hormone levels, and imaging findings[34,35]. Pituitary MRI, hormone levels, and clinical manifestations can diagnose CPP. Studies[36] have shown that pituitary MRI is highly sensitive and specific in the diagnosis of CPP in girls, and has higher accuracy than other examination methods. Other studies[37] have shown that pituitary MRI indicators, such as posterior pituitary lobe thickness, and pituitary signal abnormalities are related to treatment effects and prognosis, and can serve as an important reference for predicting patient prognosis and guiding treatment strategies. Although the likelihood of finding lesions requiring intervention is low, systematic MRI is currently the most effective diagnostic method for diagnosing occult lesions in girls with CPP. As an auxiliary examination method, pituitary MRI needs to be combined with other examination results, such as sex hormone levels and bone age assessment, to improve the accuracy of diagnosis and the reliability of comprehensive judgment[38].

Based on artificial intelligence algorithm and safety medical imaging, the application of pelvic ultrasound combined with pituitary MRI in the diagnosis of girls with CPP was analyzed. The pelvic ultrasound indexes and pituitary MRI indexes and pituitary function indexes of girls with PP and girls

with NG were compared. The results showed that the CNN algorithm had higher diagnostic sensitivity, accuracy, and specificity. The long diameter of the uterus, anteroposterior diameter of uterus, transverse diameter of uterus, ovary long diameter, ovary anteroposterior diameter, and ovary transverse diameter were larger in PP group. In the PP group, uterine volume was 1.92 cm^3, ovarian volume was 1.71 cm^3, and those in the NG was 1.19 cm^3 and 1.08 cm^3 ($p<0.05$). The largest follicle diameters were 0.73 cm and 0.25 cm in PP group and NG ($p<0.05$). Coronal height, coronal width, sagittal height, sagittal anteroposterior diameter, sagittal cross-sectional area of pituitary, MRI morphology, pituitary function parameters E_2, LH peak and FSH peak, and LH peak and/FSH peak were greater in the PP group. Pituitary MRI morphologic pituitary volumes in PP group and NG were 272.68 mm and 191.37 mm ($p<0.05$). Pelvic ultrasound combined with pituitary MRI can better diagnose PP in girls and has positive clinical value.

Conclusions

Based on the artificial intelligence algorithm, the diagnostic value of pelvic ultrasound index and pituitary MRI index for PP in girls was analyzed. It was found that pelvic ultrasound index and pituitary MRI index had positive diagnostic value for CPP girls, and CNN algorithm had better diagnostic effect and higher accuracy. Pituitary function indexes have positive reference significance for the diagnosis of PP. The shortcomings are that only ultrasound parameters and MRI parameters are explored for the diagnostic value of CPP, and no comparison is made with other examination methods. In the future, more examination methods need to be selected for the comparison of diagnostic effects, providing a reference for the prevention and control of CPP.

Informed Consent
Patients and their families signed informed consent.

Ethics Approval
The study was approved by the Medical Ethics Committee of Nantong First People's Hospital (approval No.: 2020KT093).

Conflict of Interest
The authors declare that they have no conflict of interest.

Availability of Data and Materials
The datasets used and/or analyzed during the current study are available from the corresponding author on reasonable request.

Funding
Not received.

ORCID ID
Xiaolin Gu: 0009-0008-2882-7911

Authors' Contributions
Yane Chen and Lili Shen designed the research. Xiaolin Gu and Min Xu provided critical comments and revised the manuscript. All authors contributed to the article and approved the submitted version.

References

1) Sharma DN, Izzuddeen Y. In Regard to de Paula et al. Int J Radiat Oncol Biol Phys 2021; 109: 1126-1127.
2) Fernandes CJ, Morinaga L, Alves JL Jr, Castro MA, Calderaro D, Jardim C, Souza R. Cancer-associated thrombosis: the when, how and why. Eur Respir Rev 2019; 28: 180119.
3) Zhou WX, Shen Y, Hu ET, Zhao Y, Sheng MY, Zheng YX, Wang SY, Lee YP, Wang CZ, Lynch DW, Chen LY. Nano-Cr-film-based solar selective absorber with high photo-thermal conversion efficiency and good thermal stability. Opt Express 2012; 20: 28953-28962.
4) Gandhi K, Barzegar-Fallah A, Banstola A, Rizwan SB, Reynolds J. Ultrasound-Mediated Blood-Brain Barrier Disruption for Drug Delivery: A Systematic Review of Protocols, Efficacy, and Safety Outcomes from Preclinical and Clinical Studies. Pharmaceutics 2022; 14: 833.
5) Bastard P, Gervais A, Le Voyer T, Rosain J, Philippot Q, Manry J, Michailidis E, Hoffmann HH, Eto S, Garcia-Prat M, Bizien L, Parra-Martínez A, Yang R, Haljasmägi L, Migaud M, Särekannu K, Maslovskaja J, de Prost N, Tandjaoui-Lambiotte Y, Luyt CE, Amador-Borrero B, Gaudet A, Poissy J, Morel P, Richard P, Cognasse F, Troya J, Trouillet-Assant S, Belot A, Saker K, Garçon P, Rivière JG, Lagier JC, Gentile S, Rosen LB, Shaw E, Morio T, Tanaka J, Dalmau D, Tharaux PL, Sene D, Stepanian A, Megarbane B, Triantafyllia V, Fekkar A, Heath JR, Franco JL, Anaya JM, Solé-Violán J, Imberti L, Biondi A, Bonfanti P, Castagnoli R, Delmonte OM, Zhang Y, Snow AL, Holland SM, Biggs C, Moncada-Vélez M, Arias AA, Lorenzo L, Boucherit S, Coulibaly B, Anglicheau D, Planas AM, Haerynck F, Duvlis S, Nussbaum RL, Ozcelik T, Keles S, Bousfiha AA, El Bakkouri J, Ramirez-Santana C, Paul S, Pan-Hammarström Q, Hammarström L, Dupont A, Kurolap A,

Metz CN, Aiuti A, Casari G, Lampasona V, Ciceri F, Barreiros LA, Dominguez-Garrido E, Vidigal M, Zatz M, van de Beek D, Sahanic S, Tancevski I, Stepanovskyy Y, Boyarchuk O, Nukui Y, Tsumura M, Vidaur L, Tangye SG, Burrel S, Duffy D, Quintana-Murci L, Klocperk A, Kann NY, Shcherbina A, Lau YL, Leung D, Coulongeat M, Marlet J, Koning R, Reyes LF, Chauvineau-Grenier A, Venet F, Monneret G, Nussenzweig MC, Arrestier R, Boudhabhay I, Baris-Feldman H, Hagin D, Wauters J, Meyts I, Dyer AH, Kennelly SP, Bourke NM, Halwani R, Sharif-Askari NS, Dorgham K, Sallette J, Sedkaoui SM, AlKhater S, Rigo-Bonnin R, Morandeira F, Roussel L, Vinh DC, Ostrowski SR, Condino-Neto A, Prando C, Bonradenko A, Spaan AN, Gilardin L, Fellay J, Lyonnet S, Bilguvar K, Lifton RP, Mane S, Anderson MS, Boisson B, Béziat V, Zhang SY, Vandreakos E, Hermine O, Pujol A, Peterson P, Mogensen TH, Rowen L, Mond J, Debette S, de Lamballerie X, Duval X, Mentré F, Zins M, Soler-Palacin P, Colobran R, Gorochov G, Solanich X, Susen S, Martinez-Picado J, Raoult D, Vasse M, Gregersen PK, Piemonti L, Rodríguez-Gallego C, Notarangelo LD, Su HC, Kisand K, Okada S, Puel A, Jouanguy E, Rice CM, Tiberghien P, Zhang Q, Cobat A, Abel L, Casanova JL. Autoantibodies neutralizing type I IFNs are present in ~4% of uninfected individuals over 70 years old and account for ~20% of COVID-19 deaths. Sci Immunol 2021; 6: eabl4340.

6) Klein KO, Freire A, Gryngarten MG, Kletter GB, Benson M, Miller BS, Dajani TS, Eugster EA, Mauras N. Phase 3 Trial of a Small-volume Subcutaneous 6-Month Duration Leuprolide Acetate Treatment for Central Precocious Puberty. J Clin Endocrinol Metab 2020; 105: e3660-3671.
7) Okawa N, Suyama Y, Kaji A. Reduced cleavage by sodium hydroxide of methyladenine in DNA sequencing. Nucleic Acids Res 1985; 13: 7639-7645.
8) Shen M, Zhang JQ, Zhao LL, Groenewald JZ, Crous PW, Zhang Y. Venturiales. Stud Mycol 2020; 96: 185-308.
9) Wang S, Yao H, Ding L, Gao Y, Wang P, Xue Y. Effects of High-Glucose and High-Fat Condition on Estrogen Receptor- and Sexual Precocity-Related Genes in GT1-7 Cells. Med Sci Monit 2020; 26: e922860.
10) Canton A, Latronico AC. Brain MRI in Girls With Central Precocious Puberty: A Time for New Approaches. J Clin Endocrinol Metab 2021; 106: e2806-e2808.
11) van der Spoel E, Roelfsema F, Akintola AA, Jansen SW, Slagboom PE, Westendorp R, Blauw GJ, Pijl H, van Heemst D. Interrelationships Between Pituitary Hormones as Assessed From 24-hour Serum Concentrations in Healthy Older Subjects. J Clin Endocrinol Metab 2020; 105: e1201-1214.
12) Lee JJ, Lee ST, Jung KH, Chu K, Lee SK. Anti-LGI1 Limbic Encephalitis Presented with Atypical Manifestations. Exp Neurobiol 2013; 22: 337-340.
13) Cantas-Orsdemir S, Garb JL, Allen HF. Prevalence of cranial MRI findings in girls with central precocious puberty: a systematic review and meta-analysis. J Pediatr Endocrinol Metab 2018; 31: 701-710.
14) Hirth M, Dietzel L, Steiner S, Ludwig R, Weidenbach H, And JP, Pfannschmidt T. Photosynthetic acclimation responses of maize seedlings grown under artificial laboratory light gradients mimicking natural canopy conditions. Front Plant Sci 2013; 4: 334.
15) Hedner J, Stenlöf K, Zou D, Grote L. Reply to Chen et al. Am J Respir Crit Care Med 2022; 206: 1051.
16) Peper ES, Bastiaansen J. Editorial for "Development and Validation of a Combined MRI Radiomics, Imaging and Clinical Parameter Based Machine Learning Model for Identifying Idiopathic Central Precocious Puberty in Girls". J Magn Reson Imaging 2023; doi: 10.1002/jmri.28728.
17) Kämpfer P, Glaeser SP, Soby SD. Chromobacterium pseudoviolaceum Kämpfer et al. 2009 is a later heterotypic synonym of Chromobacterium violaceum Bergonzini 1880. Int J Syst Evol Microbiol 2018; 68: 2967-2968.
18) Pucarelli I, Accardo F, Tarani L, Demiraj V, Segni M, Pasquino AM. Precocious puberty in two girls with Chiari I malformation: a contribution to a larger use of brain MRI in the diagnosis of central precocious puberty. Minerva Pediatr 2010; 62: 315-317.
19) Aldhyani T, Alkahtani H. Artificial Intelligence Algorithm-Based Economic Denial of Sustainability Attack Detection Systems: Cloud Computing Environments. Sensors (Basel) 2022; 22: 4685.
20) Sun Z, Zhang J, Yang J, Li J, Wang J, Hu X. Acclimation of 2-chlorophenol-biodegrading activated sludge and microbial community analysis. Water Environ Res 2019; 91: 273-280.
21) Taquet M, Dercon Q, Harrison PJ. Response to the letter by Lin et al. Brain Behav Immun 2022; 104: 215.
22) Stidham RW, Takenaka K. Artificial Intelligence for Disease Assessment in Inflammatory Bowel Disease: How Will it Change Our Practice. Gastroenterology 2022; 162: 1493-1506.
23) Wei X, Marussig B, Antolin P, Buffa A. Immersed boundary-conformal isogeometric method for linear elliptic problems. Comput Mech 2021; 68: 1385-1405.
24) Kagimoto A, Tsutani Y, Okada M. Reply to Zhou et al. Eur J Cardiothorac Surg 2022; 62: ezac245.
25) Faller RV. The application of in situ models for evaluation of new fluoride-containing systems. Adv Dent Res 1995; 9: 290-299; discussion 300-303.
26) Mogensen SS, Aksglaede L, Mouritsen A, Sørensen K, Main KM, Gideon P, Juul A. Pathological and incidental findings on brain MRI in a single-center study of 229 consecutive girls with early or precocious puberty. PLoS One 2012; 7: e29829.
27) Torres-Tamayo M, Zurita-Cruz JN, Aguilar-Herrera BE, Miranda-Lora AL, Calzada-León R, Rivera-Hernández AJ, Morales-Pérez MA, Padrón-Martínez MM, Ruiz-Reyes ML, García-Morales LM, Barrón-Uribe C, Arguinzoniz-Valenzuela SL, Torres-Castañeda MC, Lizárraga-Paulin L, Núñez-Hernández JA, Cornejo-Barrera J, Vidal-González MT, Martínez-Alvarado MR, Nishimura-Meguro E, Bravo-Ríos LE, Garrido-Magaña EP, Orozco-Morales JA, Medina-Bravo PG, Coyote-Estrada N, Castilla-Peón MF. Puberty blockade: Clinical guideline for the diagnosis and treatment of precocious puberty. Bol Med Hosp Infant Mex 2020; 77: 19-25.

28) Vaidya A, Carey RM. Evolution of the Primary Aldosteronism Syndrome: Updating the Approach. J Clin Endocrinol Metab 2020; 105: 3771-3783.
29) Sasaki Y, Hamada K, Kaneta T, Takahashi T, Kubota Y, Ishida H, Ichikawa W. Is repeating FOLFIRINOX in the original dosage and treatment schedule tolerable in Japanese patients with pancreatic cancer. Cancer Sci 2015; 106: 1100.
30) Durá-Travé T, Ortega Pérez M, Ahmed-Mohamed L, Moreno-González P, Chueca Guindulain MJ, Berrade-Zubiri S. Central precocious puberty in girls: Diagnostic study and auxological response to triptorelin treatment. Endocrinol Diabetes Nutr (Engl Ed) 2019; 66: 410-416.
31) Zou P, Zhang L, Zhang R, Wang C, Lin X, Lai C, Lu Y, Yan Z. Development and Validation of a Combined MRI Radiomics, Imaging and Clinical Parameter-Based Machine Learning Model for Identifying Idiopathic Central Precocious Puberty in Girls. J Magn Reson Imaging 2023; doi: 10.1002/jmri.28709.
32) Ng SM, Kumar Y, Cody D, Smith CS, Didi M. Cranial MRI scans are indicated in all girls with central precocious puberty. Arch Dis Child 2003; 88: 414-418; discussion 414-418.
33) Ramirez-Valles J. The New HE&B Editorial Team. Health Educ Behav 2018; 45: 309-310.
34) Giacomozzi L, Kjær C, Brøndsted Nielsen S, Ashworth EK, Bull JN, Stockett MH. Non-statistical fragmentation in photo-activated flavin mononucleotide anions. J Chem Phys 2021; 155: 044305.
35) Stagi S, Galluzzi F, Bindi G, Lapi E, Cecchi C, Salti R, Chiarelli F. Precocious puberty in a girl with floating-harbor syndrome. J Pediatr Endocrinol Metab 2007; 20: 1333-1337.
36) Lucas SM. Editorial comment for Cho et al. J Endourol 2013; 27: 11-12.
37) Zinman B, Wanner C, Lachin JM, Fitchett D, Bluhmki E, Hantel S, Mattheus M, Devins T, Johansen OE, Woerle HJ, Broedl UC, Inzucchi SE. Empagliflozin, Cardiovascular Outcomes, and Mortality in Type 2 Diabetes. N Engl J Med 2015; 373: 2117-2128.
38) Varimo T, Huttunen H, Miettinen PJ, Kariola L, Hietamäki J, Tarkkanen A, Hero M, Raivio T. Precocious Puberty or Premature Thelarche: Analysis of a Large Patient Series in a Single Tertiary Center with Special Emphasis on 6- to 8-Year-Old Girls. Front Endocrinol (Lausanne) 2017; 8: 213.